N92-21913

GAMMA-RAY BURST ASTROMETRY II: NUMERICAL TESTS

L. G. TAFF and S. T. HOLFELTZ
SPACE TELESCOPE SCIENCE INSTITUTE
3700 San Martin Drive
Baltimore, MD 21218

Since the announcement of the discovery of sources of bursts of gamma-ray radiation in 1973, many more reports of such bursts have been published. Numerous artificial satellites have been equipped with gamma-ray detectors including GRO. Unfortunately, we have made almost no progress in identifying the sources of this high energy radiation. Only one visible counterpart is known. We suspect that this is a consequence of the methods currently used to define gamma-ray burst source 'error boxes'. An alternative procedure was proposed in 1988 by Taff. In the current paper we report on Monte Carlo simulations of the efficacy of this technique using realistic burst timing uncertainties and satellite location errors as well as a variety of satellite constellations. Since these are controlled numerical experiments, we can examine the dependence of the statistics of the errors in the deduced burst wavefront normal as a function of the timing inconsistencies, detector location standard deviations, and especially the number and distribution of the detectors. The results clearly show that an arc minute prediction of a unique burst location is routinely obtainable once there are at least two interplanetary detectors.

I. INTRODUCTION

An alternative to the customary "time difference of arrival" method of gamma-ray burst source location was presented by Taff in 1988. This technique predicts a unique location for the source of the burst independent of the number of different gamma-ray detectors registering the burst. All the detector locations and times of observation are folded into a single, simple computation. In contrast, the standard method only defines a (circular) locus of points on the celestial sphere on which the burst source location should reside. When there are multiple detections of the same burst, a finite area on the celestial sphere is, in practice, delineated via a pair-wise analysis of the location and timing data. With real data—and with a very difficult problem of time registration of bursts observed with detectors of different responsivities and sensitivities, spacecraft clock errors, timing errors arising from binning the recorded photons, differing thresholds before recording is initiated, and so forth—the geometrically pure problem is degraded into one whose best possible outcome is that all the intersection points lie near each other. This small area is used to define an 'error-box' in which the burst source is thought to lie (see Fig. 1).

The location deduced in this fashion will, in general, not be the statistically most likely position for the source of the burst. The hope that the circle drawn for each pair of detecting sensors is centered in a region of high source location probability will not be consistently realized in practice; indeed, the circle must lie completely outside the one-sigma error region fairly often. Furthermore, the supposition of a probabilistically uniform region surrounding

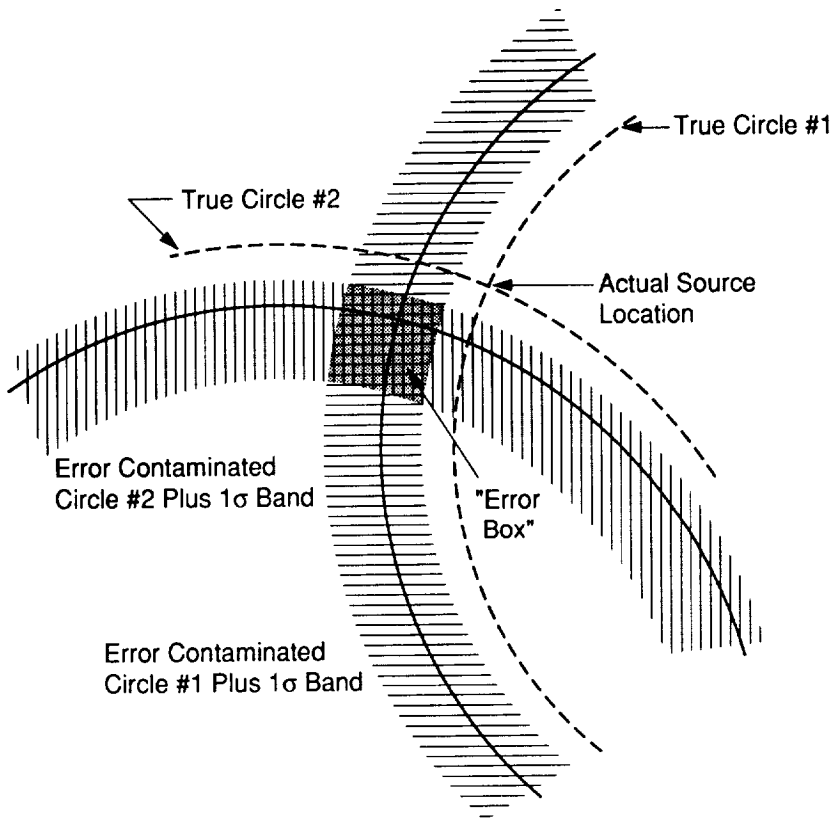

Fig. 1. General intersection area for "time difference of arrival" gamma-ray burst source location determination. Note error bands need not be symmetrically placed relative to circular locus nor include the true circle.

the most probable source location circle may be too simplistic—it is not clear that the underlying probability function is that well-behaved.

Finally, *random* errors in detector location became *systematic* errors in the "time difference of arrival" method circle (see Fig. 2; timing errors change the radius of the circle). In Fig. 2 the random error in the location of the spacecraft at P causes us to place it at P' instead. This alters the axis of the cone from OP to OP' thereby systematically shifting the locus of possible source locations. Similarly, a random error in the relative timing between the two spacecraft will cause θ to be over-estimated or under-estimated thereby systematically enlarging or decreasing the locus of possible source locations. One could compute the one-sigma regions in an attempt to produce reliable error estimates. However, none have been published and the amount of computation necessary for the customary method must exceed that necessary to similarly characterize the results of Taff's method by the ratio of (number of points in a circle):one since this is the ratio of their prediction volumes. Hence, such a calculation would be unwieldy and extremely expensive computationally. A more complete comparison between the different aspects of the two methods is given in Table 1.

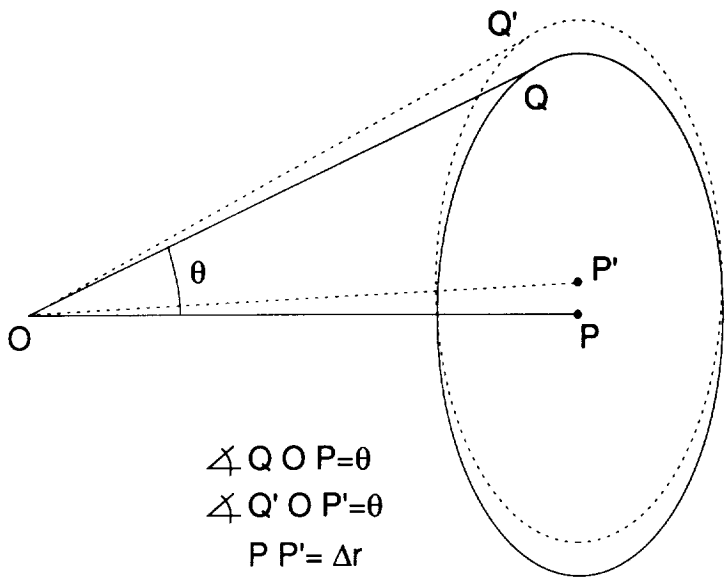

Fig. 2. Locus of potential burst source locations systematically shifted by the random spacecraft positional error PP'.

TABLE 1. COMPARISON OF THE TWO METHODS

ASPECT	TAFF'S METHOD	CUSTOMARY METHOD
PREDICTS A UNIQUE LOCATION	YES	NO
SIMULTANEOUSLY USES ALL THE OBSERVATIONAL DATA	YES	NO
SUBSUMES THE OTHER METHOD AS A SPECIAL CASE	YES	NO
IS EASILY AMENABLE TO MONTE CARLO SIMULATION	YES	NO
CAN EASILY ASSESS THE QUALITY OF THE PREDICTION	YES	NO

The technique developed in Taff (1988) is easily amenable to numerical simulation. This paper reports on extensive Monte Carlo computations of its predictions for the location of gamma-ray bursts. These calculations explore ranges of numbers of potential spacecraft-carrying burst detectors, in cislunar (2, 3, or 4) and interplanetary (1, 2, 3, or 4) space, and all 4π steradians of potential burst source locations. In addition, because these are controlled numerical experiments, we can statistically characterize both the accuracy and the precision of the results. In sum, they conclusively show that a minute of arc is routinely available once there are two interplanetary spacecraft in the burst detection network.

In the next section we briefly review the fundamental ideas behind this method. The third section of the paper describes the Monte Carlo simulations we have performed. Comments on our oral presentation have defined additional areas of research; these are outlined in the fourth section. Because of the closeness of the Huntsville meeting, we shall report there on these additional topics. These will include more realistic simulations and analytical progress on solving our form of the problem. Using our software, within a year an entirely new catalog of burst source locations, for every gamma-ray burst multiply detected, could be computed. Moreover, each new source location would be described by a reliable error estimate (once access to the data is obtained).

II. CONCEPT

The essential concept behind the technique is to use the one piece of information about the gamma-ray burst that we indisputedly know; to wit, that the phase of the burst (whether planar or spherical) is an invariant for all the detectors. Could the detectors on the interplanetary burst network measure the phase ϕ of the burst wavefront, they would all obtain the same value (absent observational errors of course), namely

$$\phi = \mathbf{k} \cdot \mathbf{r} - \omega t \tag{1}$$

where $\mathbf{r}$ is the solar system barycentric location of the spacecraft, t is the time of arrival of the burst at that spacecraft (t is assumed to be a shared inertial timescale), $\mathbf{k}$ is the wave vector of the burst wavefront, and ω is the angular frequency of the burst ($= 2\pi\nu$ where ν is the frequency of the photon; $\nu = c/\lambda$ where c is the speed of light in vacuo and λ is the wavelength of the burst). Rewriting $\mathbf{k}$ as $k\mathbf{u}$, where $\mathbf{u}$ is the wavefront normal, the pseudo-invariant Φ can be defined, viz.

$$\Phi = \mathbf{u} \cdot \mathbf{r} - ct. \tag{2}$$

Although neither ϕ nor Φ can be directly measured, they do include all the observational data at our disposal and the quantity we want to determine — $\mathbf{u}$. Taff's (1988) concept was, that especially in the presence of unknown systematics and the very difficult time registration problem we have, enforcing the constraint that each sensor's (albeit unknown and unmeasurable) value of Φ be the same would lead to a mathematically well-posed problem for the computation of $\mathbf{u}$. The explicit method Taff (1988) proposed for doing so was to minimize the quantity

$$T = \frac{1}{2} \sum_{n,m=1}^{N} (\Phi_n - \Phi_m)^2 \tag{3}$$

subject to the constraint that $\mathbf{u} \cdot \mathbf{u} = 1$. Taff suggested that the constraint be incorporated via a Lagrange multiplier.

By explicit computation, Taff (1988) further showed that the customary time of arrival analysis was contained in this principle as a special case of minimizing Eq. (3) (*i.e.,* they are represented by the cases of $N = 2$ and $N = 3$). Taff also explicitly computed the coplanar solution for $\mathbf{u}$ when N was equal to 4.

III. MONTE CARLO SIMULATIONS

The only drawback of the first paper was that it did not contain any numerical testing of this novel form of statistical estimation. This defect will be repaired immediately.

Since many of the gamma-ray bursts detected in the past have involved at least two near-Earth (*i.e.,* within cislunar space) detectors and at least one interplanetary detector, this formed the minimum configuration for our simulations. All configurations of $N_{close} = 2$, 3, or 4 and $N_{far} = 1$, 2, 3, or 4 have been considered. Not surprisingly, the algorithm works much better once N_{far} is at least two.

In addition to considering two groups of spacecraft, we considered a bifurcated distribution of spacecraft location uncertainties. For those in near-Earth orbit location uncertainties of 100 or 200 km were allowed (that is to the actual location of the spacecraft we added a vector for which each component was normally distributed about zero with a standard deviation of 100 or 200 km in length). For those spacecraft in interplanetary space we used the larger values of 1000 and 2000 km to span likely uncertainties. Finally, we also had to assign timing errors. These represent a convolution of spacecraft clock errors, detection timing (*e.g.,* binning), sensor-to-sensor correlation, and so on. We used standard deviations of 25 and 50 milli-seconds coupled with the zero mean normal distribution to represent these errors. Note that 25 milli-seconds represents 7500 km at the speed of light. Hence, since spacecraft locations are bound to improve, timing errors will continue to dominate the problem.

The spacecraft were always coplanar, in the plane of the ecliptic. This is a very good (numerical) approximation to the real case and significantly simplifies the (analytic aspects of the) computations. Spacecraft in cislunar space where deposited uniformly in azimuth relative to the Earth-Sun line and uniformly in distance between geosynchronous distance (42,000 km) and the mean lunar distance (400,000 km). Similarly, the interplanetary spacecraft were uniformly distributed in azimuth relative to the Earth-Sun line and uniformly in heliocentric distance between 0.5 and 4 A. U.

Once the standard deviations of the locations and timing were set, and the numbers of spacecraft fixed, the spacecraft were strewn across the solar system. For this constellation of spacecraft we then chose 100 different unit wavefront normal vectors to represent the gamma-ray burst ($\mathbf{n}$). These were uniformly distributed over the celestial sphere. We next computed the relative timings, corrupted the spacecraft locations and timings as described above, and solved for $\mathbf{u}$. The angle θ, given by the scalar product between $\mathbf{n}$ and $\mathbf{u}$,

$$\cos\theta = \mathbf{n} \cdot \mathbf{u} \tag{4}$$

tells us the angular mis-distance between the actual direction of gamma-ray burst source and the calculated one (note that the direction of the gamma-ray burst source is $-\mathbf{n}$ and the computed direction is $-\mathbf{u}$). Another way to think of θ is that it is the 3σ radius of our error

TABLE 2. RESULTS OF MONTE CARLO SIMULATIONS

N_{close}	N_{far}	$\sigma_{r_{close}}$ (km)	$\sigma_{r_{far}}$ (km)	σ_t (msec)	$\langle\theta\rangle$ (′)	σ_θ (′)	$\sigma_{r_{close}}$ (km)	$\sigma_{r_{far}}$ (km)	$\langle\theta\rangle$ (′)	σ_θ (′)
2	1	10	100	25	452.60	380.60	100	1000	359.20	333.80
2	2	10	100	25	1.26	2.45	100	1000	2.50	4.20
2	3	10	100	25	0.88	1.51	100	1000	0.87	1.50
2	4	10	100	25	0.84	1.34	100	1000	0.81	1.32
3	1	10	100	25	107.60	123.30	100	1000	112.10	130.20
3	2	10	100	25	1.60	2.88	100	1000	4.14	6.31
3	3	10	100	25	0.81	1.31	100	1000	0.80	1.33
3	4	10	100	25	0.79	1.20	100	1000	0.78	1.16
4	1	10	100	25	81.12	100.10	100	1000	75.77	91.00
4	2	10	100	25	1.87	3.29	100	1000	4.63	7.10
4	3	10	100	25	0.83	1.39	100	1000	0.68	1.10
4	4	10	100	25	0.73	1.16	100	1000	0.77	1.19
2	1	20	100	25	542.30	460.40	200	1000	467.80	427.80
2	2	20	100	25	1.66	2.59	200	1000	11.70	22.05
2	3	20	100	25	0.90	1.53	200	1000	0.83	1.44
2	4	20	100	25	0.76	1.15	200	1000	0.70	1.13
3	1	20	100	25	119.60	138.40	200	1000	121.20	137.60
3	2	20	100	25	2.36	4.03	200	1000	2.06	3.94
3	3	20	100	25	0.77	1.33	200	1000	0.80	1.39
3	4	20	100	25	0.73	1.16	200	1000	0.73	1.16
4	1	20	100	25	72.86	90.62	200	1000	71.43	93.99
4	2	20	100	25	1.30	2.48	200	1000	1.25	2.25
4	3	20	100	25	0.76	1.24	200	1000	0.75	1.32
4	4	20	100	25	0.76	1.23	200	1000	0.72	1.15
2	1	10	200	25	370.20	324.70	100	2000	397.40	370.80
2	2	10	200	25	2.37	4.07	100	2000	1.45	2.66
2	3	10	200	25	0.75	1.24	100	2000	0.84	1.49
2	4	10	200	25	0.73	1.13	100	2000	0.74	1.22
3	1	10	200	25	123.80	141.10	100	2000	115.70	133.10
3	2	10	200	25	2.72	5.21	100	2000	1.15	2.12
3	3	10	200	25	0.81	1.39	100	2000	0.80	1.27
3	4	10	200	25	0.75	1.22	100	2000	0.76	1.29
4	1	10	200	25	72.13	93.13	100	2000	82.14	105.50
4	2	10	200	25	1.85	3.41	100	2000	1.64	2.95
4	3	10	200	25	0.79	1.32	100	2000	0.76	1.37
4	4	10	200	25	0.71	1.16	100	2000	0.77	1.17
2	1	20	200	25	491.50	423.50	200	2000	442.70	401.00
2	2	20	200	25	2.98	4.31	200	2000	3.29	4.67
2	3	20	200	25	0.77	1.29	200	2000	0.81	1.34
2	4	20	200	25	0.77	1.19	200	2000	0.72	1.16
3	1	20	200	25	116.60	126.70	200	2000	124.30	143.50

Table 2. *Continued.*

N_{close}	N_{far}	$\sigma_{r_{close}}$ (km)	$\sigma_{r_{far}}$ (km)	σ_t (msec)	$\langle\theta\rangle$ ($'$)	σ_θ ($'$)	$\sigma_{r_{close}}$ (km)	$\sigma_{r_{far}}$ (km)	$\langle\theta\rangle$ ($'$)	σ_θ ($'$)
3	2	20	200	25	2.68	4.20	200	2000	2.07	4.15
3	3	20	200	25	0.75	1.22	200	2000	0.87	1.42
3	4	20	200	25	0.72	1.14	200	2000	0.84	1.30
4	1	20	200	25	72.60	92.00	200	2000	76.02	92.77
4	2	20	200	25	1.66	2.99	200	2000	1.34	2.77
4	3	20	200	25	0.80	1.32	200	2000	0.81	1.35
4	4	20	200	25	0.83	1.30	200	2000	0.78	1.21
2	1	10	100	50	685.60	575.30	100	1000	718.70	615.70
2	2	10	100	50	2.27	4.89	100	1000	6.35	9.42
2	3	10	100	50	1.01	1.76	100	1000	1.14	1.99
2	4	10	100	50	0.86	1.38	100	1000	0.92	1.49
3	1	10	100	50	227.80	219.50	100	1000	197.90	195.20
3	2	10	100	50	2.84	4.77	100	1000	3.02	4.81
3	3	10	100	50	1.07	1.86	100	1000	1.02	1.78
3	4	10	100	50	0.89	1.39	100	1000	0.78	1.27
4	1	10	100	50	137.20	147.90	100	1000	128.90	138.20
4	2	10	100	50	2.10	3.95	100	1000	2.44	4.03
4	3	10	100	50	1.00	1.61	100	1000	0.97	1.78
4	4	10	100	50	0.84	1.30	100	1000	0.80	1.37
2	1	20	100	50	729.50	605.20	200	1000	616.50	536.50
2	2	20	100	50	1.93	3.67	200	1000	3.89	5.74
2	3	20	100	50	0.99	1.55	200	1000	1.10	1.93
2	4	20	100	50	0.97	1.50	200	1000	0.88	1.37
3	1	20	100	50	208.10	197.20	200	1000	206.10	199.50
3	2	20	100	50	1.95	3.39	200	1000	2.43	4.67
3	3	20	100	50	0.96	1.62	200	1000	0.95	1.67
3	4	20	100	50	0.93	1.43	200	1000	0.80	1.23
4	1	20	100	50	152.10	157.70	200	1000	148.10	154.90
4	2	20	100	50	3.50	5.09	200	1000	2.15	3.81
4	3	20	100	50	0.93	1.61	200	1000	1.00	1.63
4	4	20	100	50	0.94	1.44	200	1000	0.82	1.31
2	1	10	200	50	662.60	560.00	100	2000	617.80	534.40
2	2	10	200	50	3.73	5.66	100	2000	2.31	4.11
2	3	10	200	50	0.99	1.70	100	2000	1.06	1.76
2	4	10	200	50	0.98	1.57	100	2000	0.91	1.41
3	1	10	200	50	235.40	224.40	100	2000	194.50	192.70
3	2	10	200	50	2.66	4.03	100	2000	2.47	4.40
3	3	10	200	50	1.05	1.75	100	2000	0.94	1.52
3	4	10	200	50	0.90	1.53	100	2000	0.82	1.26
4	1	10	200	50	116.00	125.50	100	2000	164.40	173.10
4	2	10	200	50	3.32	5.96	100	2000	3.30	4.93

Table 2. *Continued.*

N_{close}	N_{far}	$\sigma_{r_{close}}$ (km)	$\sigma_{r_{far}}$ (km)	σ_t (msec)	$\langle\theta\rangle$ (′)	σ_θ (′)	$\sigma_{r_{close}}$ (km)	$\sigma_{r_{far}}$ (km)	$\langle\theta\rangle$ (′)	σ_θ (′)
4	3	10	200	50	0.91	1.64	100	2000	0.97	1.62
4	4	10	200	50	0.87	1.50	100	2000	0.85	1.44
2	1	20	200	50	653.10	550.60	200	2000	530.40	472.00
2	2	20	200	50	12.94	13.02	200	2000	2.44	4.55
2	3	20	200	50	1.10	1.86	200	2000	1.13	2.05
2	4	20	200	50	0.87	1.35	200	2000	0.90	1.46
3	1	20	200	50	220.30	209.80	200	2000	215.00	216.00
3	2	20	200	50	4.96	6.59	200	2000	2.92	5.19
3	3	20	200	50	1.03	1.90	200	2000	0.96	1.76
3	4	20	200	50	0.89	1.46	200	2000	0.80	1.25
4	1	20	200	50	144.50	150.40	200	2000	138.30	151.40
4	2	20	200	50	1.96	3.45	200	2000	1.71	3.03
4	3	20	200	50	0.92	1.55	200	2000	1.06	1.90
4	4	20	200	50	0.82	1.34	200	2000	0.81	1.36

circle. By averaging over the 100 randomly chosen wavefront normals, and then again over 100 different constellations of the same set of sensors, we can unambiguously demonstrate the power of the technique. These results are given in the right-hand portion of Table 2 for the larger location uncertainties.

Table 2's mid-section has the identical format to its right-hand portion except that all the location uncertainties have been reduced by an order of magnitude (*i.e.*, 10 and 20 km for spacecraft in cislunar space and 100 and 200 km for those in interplanetary space). Clearly, once there are at least two detectors located in interplanetary space an arc minute is the routine performance of the technique. Finally, since we do know the true location of the burst source, we can also compute the standard deviation about the mean [which is necessarily non-zero owing to the form in Eq. (4)]. These values are also in Table 2 (*i.e.*, σ_θ).

IV. ADDITIONAL AREAS OF RESEARCH

One consequence of the oral presentation of these results were the following suggestions for future work: (1) Simulations tailored to the Ulysses, Pioneer-Venus Orbiter, GRO, and GRANAT configuration; (2) More analytical work in describing the error distribution of this method, and (3) Simulations of the BATSE instrument alone as a gamma-ray burst source location detector. These additional computations will be reported on in paper III to be given at the Huntsville Gamma-Ray Burst Workshop.

Reference

Taff, L. G., 1988, Ap J 326, 1032